Petroleum Science 23 (2026) 3506–3518

Contents lists available at ScienceDirect

Petroleum Science

journal homepage: www.keaipublishing.com/en/journals/petroleum-science

Original Paper

Performance of multifunctional viscous slickwater for enhanced oil recovery in tight oil reservoirs

Tian-Bo Liang *, Jun-Lin Wu, Zi-Lin Deng, Shuai Yuan, Hao Liu, Bin Wang, Fu-Jian Zhou

State Key Laboratory of Petroleum Resources and Engineering, China University of Petroleum (Beijing), Beijing, 102249, China

ARTICLE INFO

Article history:
Received 2 August 2025
Received in revised form
13 January 2026
Accepted 13 January 2026
Available online 17 January 2026

Edited by Yan-Hua Sun

Keywords:
Viscous slickwater
Hydraulic fracturing
Enhanced oil recovery
Wettability alteration
Viscoelasticity
Tight oil reservoirs

ABSTRACT

Economically recovering oil from tight/shale reservoirs requires extensively developed propped fracture networks and rock matrix with sufficient oil mobility, which imposes higher demands on the fracturing fluid. This study develops a DME-aided viscous slickwater (MEVS) that addresses these dual challenges. During hydraulic fracturing, DME reinforces viscoelasticity through the hydrophobic association, significantly improving the proppant-carrying capacity without substantially increasing viscosity, thereby enabling the creation of extensive propped hydraulic fractures. After hydraulic fracturing, DME minimizes surfactant adsorption and deepens wettability alteration, thereby enlarging the water-wet zone of rock matrix to enhance oil recovery via imbibition and increased oil relative permeability. Laboratory evaluations using a visualized rough fracture model reveal that the fluid elasticity can be quantified using the Weissenberg number, which is then used to predict the proppant transport performance at a specific flow condition during hydraulic fracturing. *In-situ* NMR and pressure transmission tests confirm that DME can mobilize oil in different-sized pores from the tight rock and significantly enhance oil recovery through water imbibition, meanwhile accelerating the pressure propagation by two orders of magnitude and enlarging the surfactant-modified zone. Field applications demonstrate that MEVS can successfully carry 400 kg/m^3 proppants at 10 m^3/min without plugging issues, and triple oil production comparing to wells using the conventional slickwater. This work establishes an integrated fracturing-EOR approach and provides a laboratory-based method to optimize the pumping schedule in field operations.

1. Introduction

Tight oil reservoirs typically have low permeabilities that require horizontal drilling and hydraulic fracturing to achieve economical production rates. Among different types of fracturing fluids, slickwater can reduce the flow friction along the wellbore by more than 75% that enables a large pumping rate during hydraulic fracturing. This large pumping rate not only allows a high proppant concentration that reduces the operation time and cost, but also generates a complex fracture network that can enhance the well productivity (Raterman et al., 2017; Shrivastava et al., 2018; Gale et al., 2021).

In recent years, along with the development of deeper and more complex reservoirs, proppant usage is increasing per unit length of stimulation, which has been increased up to 2–3 t/m in tight oil or shale gas reservoirs and 3–5 t/m in shale oil reservoirs (Lei et al., 2022, 2023). Meanwhile, when cheaper local sands are used to substitute ceramic proppants, a larger proppant concentration within hydraulic fractures is required (Zhang et al., 2022). For such an increasing need of proppants, the conventional slickwater requires a longer pumping time due to its limited proppant-carrying ability, which in turn makes the slickwater less economical and environment-friendly. On the other hand, increasing water usage can potentially cause rock softening, clay swelling, or fine migration in water-sensitive reservoirs, which can reduce the permeability of the reservoir rock and the conductivity of the propped fractures (Yuan et al., 2016; Zhang et al., 2016; Li et al., 2023; Wang et al., 2023). Meanwhile, the invaded water can also cause the phase trapping or water blocking that reduces the relative permeability of the reservoir rock to hydrocarbon

* Corresponding author.
E-mail address: btliang@cup.edu.cn (T.-B. Liang).
Peer review under the responsibility of China University of Petroleum (Beijing).

https://doi.org/10.1016/j.petsci.2026.01.015
1995-8226/

(Longoria et al., 2017; Liang et al., 2018); either above reduces the well productivity after hydraulic fracturing. Therefore, the fracturing fluid with a better proppant-carrying ability is needed to increase the proppant usage while reducing the water usage during hydraulic fracturing.

Crosslinked gel using guar or its derivatives, as the other type of widely used fracturing fluid, has a larger viscosity and a better proppant-carrying ability than slickwater. However, studies have shown that broken residues of the crosslinked gel can plug the propped fractures or cover fracture faces, leading to more significant formation damage than the slickwater (Xu et al., 2011; Ouyang et al., 2012; Barati and Liang, 2014). Currently, the reverse-hybrid fracturing method is widely used in China, where a small amount of crosslinked gel is firstly pumped to initiate hydraulic fractures, followed by the slickwater pumping with proppant concentrations of typically below 300 kg/m^3, and then followed by the crosslinked-gel pumping with proppant concentrations of typically below 600 kg/m^3 (Liang et al., 2021). In this type of fracturing method, although the crosslinked gel only accounts for less than 30% of the total volume of the fracturing fluid, the formation damage due to residues of the broken gel cannot be avoided; besides, proppant plugging due to the limited proppant-carrying ability of the slickwater remains unsolved that can limit the efficiency of pumping proppants during the field operation.

Due to limitations of the conventional slickwater and the crosslinked gel, viscous slickwater has been developed and is gradually substituting the above two types of fracturing fluids in North America since 2016, especially the crosslinked gel (Poppel, 2020; Lei et al., 2022). Using linear polymers, the viscous slickwater can reduce the friction along the wellbore during hydraulic fracturing as the conventional slickwater; meanwhile, its viscosity can increase fast with the polymer concentration and thus meet the field requirement of continuous proppant-pumping without changing the fluid (Ba Geri et al., 2019c). The emergence of viscous slickwater significantly simplifies the field operation and can make the AI-assisted hydraulic fracturing possible in the near future.

Linear polymers typically show viscoelastic properties that the fluid behaves like a solid at a small shear rate and like a liquid at a large shear rate. Such viscoelasticity is typically characterized using a pair of storage and loss modulus curves changing with the shear rate; in the left region of the intersection point of two curves where the shear rate is small, loss moduli are larger than storage moduli and the proppant-carrying ability is more attributed to the fluid viscosity; on the right region of the intersection point where the shear rate is large, storage moduli are larger than loss moduli and the proppant-carrying ability is more attributed to the fluid elasticity (Gomaa et al., 2015b; Hu et al., 2015a). Currently, researchers mainly use the location of the intersection point of storage and loss modulus curves to show the viscoelasticity of viscous slickwater, where the larger the shear rate of the intersection point, the better the fluid viscoelasticity and proppant-carrying ability (Gomaa et al., 2015b; Wang et al., 2020b; Biheri and Imqam, 2022). Studies have shown that better viscoelasticity can significantly reduce the settling rate of proppants at the condition when the shear rate is larger than the intersection point of modulus curves (Hu et al., 2015b, 2015c); furthermore, when the viscoelasticity of polymers is reduced due to gel breakers or high salinity, a significant reduction in proppant-carrying ability of the viscous slickwater has been observed (Gomaa et al., 2015a; Ba Geri et al., 2019a). Using an environmental scanning electron microscope (ESEM) or a transmission electron microscope (TEM), the microstructure of viscous slickwater has been observed that the elastic energy can be stored and released through polymer stretching; this can likely enhance the proppant-carrying performance of the viscous slickwater and enable proppants to migrate far within the created fracture network during hydraulic fracturing (Bai et al., 2021; Yuan et al., 2023). However, the intersection point of two modulus curves can only qualitatively characterize the effect of viscoelasticity on proppant-carrying, since moduli do not directly reflect the magnitude of force acting on proppant-carrying of the fracturing fluid. For the viscoelastic fluid, the Weissenberg number has been used to quantify the ratio of the elastic force to the viscous force on proppant settling (Malhotra and Sharma, 2011; Thompson and Oishi, 2021). In the steady simple shear flow regime, which is a fair assumption for the slurry flow carried by a viscoelastic fluid within hydraulic fractures, the Weissenberg number is calculated by the first normal-stress difference (which determines the dominant elastic force) to the shear stress (which determines the viscous force), which can be simplified to twice the product of the relaxation time of the viscoelastic polymer and the shear rate (Poole, 2012). A study has shown that the Weissenberg number increases from a non-viscoelastic fluid (linear guar) to a viscoelastic fluid (viscous slickwater) at the same flow condition, and the Weissenberg number is larger than a few hundred when the viscous slickwater prevents proppants from settling without a horizontal flow (Ba Geri et al., 2019b). To ensure a successful hydraulic fracturing job with as large a concentration of proppants in the viscoelastic fluid as possible, it is necessary to establish a quantitative correlation between the Weissenberg number and the proppant-carry threshold of this viscoelastic fluid, especially within a hydraulic fracture.

To simulate the slurry flow in a hydraulic fracture, a relatively large-scale transparent fracture-flow apparatus has been used to observe the proppant migration and proppant-bank formation therein, whose size can be as tall as 1.2 m and as long as 1.8 m (Rein et al., 1993; Beason and Fagan, 1995; Anschutz et al., 2019). Using such an apparatus, the settling rate of proppants in the Newtonian fluid has been measured, from which a modified Stokes equation is established to capture the impacts of fracture width, proppant size and concentration on the settling rate of proppants (Malhotra et al., 2014; Blyton et al., 2018; He et al., 2022). This equation can be further applied in a fracture propagation simulator to predict the growth of propped fractures during hydraulic fracturing (Hu et al., 2018; Wang and Sharma, 2018). However, when the non-Newtonian fluid (like a viscoelastic fluid) is tested in this fracture-flow apparatus, studies have found that the settling rate of proppants is reduced compared with that predicted by the modified Stokes equation, and the difference seems increasing with the inner-fracture flow rate of fluid (Malhotra et al., 2014; Wang et al., 2023). In a recent large-scale fracture-flow study, it has been confirmed that the viscoelasticity of the fracturing fluid can reduce the settling rate of proppants at a large shear of above 10 s^{-1} (Biheri and Imqam, 2022). However, the inner fracture flow rate of the mimicked slurry is 0.013–0.015 m/s, which is 1–2 orders of magnitudes lower than that in the field. Therefore, it is necessary to determine the proppant-carrying threshold under different mimicked fracturing conditions to guide and optimize field operations whiling avoiding the risk of proppant plugging. Furthermore, it is also necessary to correlate the proppant-carrying ability of the viscoelastic fluid to its rheology and viscoelasticity. Such a correlation would allow the prediction of proppant transport performance based on laboratory measurements of fluid properties.

Besides the limitation of proppant-carrying ability of the fracturing fluid that results in a low conductivity of the hydraulic fracture network, tight rocks typically have permeabilities as low as a few microDarcies and the rock surface tends to be oil-wet due to adsorbed polar compounds from crude oil; both above can hinder the imbibition of fracturing fluid into pores to displace the oil therein, and limit the oil recovery rate of tight oil reservoirs to as low as 5%–10% (Liang et al., 2021). Although wettability-alteration surfactants have been widely studied and applied in conventional carbonate reservoirs, tight rocks have a significant large surface area that can adsorb surfactants, which limits the effective depth of conventional wettability-alteration surfactants and makes them uneconomical in tight oil reservoirs. Authors have developed a new type of surfactants, which are pre-synthesized into thermodynamically-stable oil-in-water microemulsions with alkenes and cosolvents; then, microemulsions can be directly mixed with the fracturing fluid for hydraulic fracturing with a concentration of 0.08%–0.1% (Liang et al., 2021; Zhao et al., 2021). Experiments have indicated that such diluted microemulsions (DME) have an average particle size of around 10 nm, and their adsorption rates is only around 1 mg/g in tight rocks with permeabilities of less than 1 mD. Compared with the conventional wettability-alteration surfactants, the adsorption rate of DME is reduced by 1–2 orders of magnitude, which ensures the economic efficiency of field operations; in a pilot test with two pairs of neighboring wells in a tight conglomerate oil reservoir, an enhanced oil recovery of more than 10% is observed in wells using the DME (Liang et al., 2021). Recent studies have also indicated that mixing with 0.08%–0.10% DME can further increase the viscosity of the viscous slickwater by more than 30% when hydrophobic monomers are implanted in polymer chains of the viscous slickwater (Bai et al., 2021; Yuan et al., 2023). Therefore, the synergic effect of the viscoelastic fluid and DME on both proppant-carrying and enhanced oil recovery needs to be elucidated.

In brief, the economic and effective development of tight oil reservoirs has put forward a higher requirement for the fracturing fluid, where the enhanced oil recovery needs to be integrated into the hydraulic fracturing process. The multifunctional viscous slickwater proposed by this study enables a friction reduction rate of over 75% at a low polymer concentration, while the hydrophobic association between DME and polymers enables the proppant-carrying ability of the viscous slickwater to reach that of the conventional guar at a large polymer concentration; more importantly, the DME component has a low adsorption rate on rock surface that a low dosage in the fracturing fluid can effectively alter the rock wettability and significantly enhance oil recovery through imbibition. In this work, the inner-fracture shear rate at the condition of hydraulic fracturing is derived from the measured rheological properties of the viscous slickwater; then, the Weissenberg number is calculated from the shear rate and used to quantify the viscoelasticity of the viscous slickwater, instead of typically used storage and loss modulus curves. Comparing with results from visualized proppant-carrying tests within a rough fracture, a threshold of Weissenberg number has been proposed that can be used to quantitatively characterize the proppant-carrying ability of the viscous slickwater at certain proppant and polymer concentrations during hydraulic fracturing. This work not only proposes an avenue to achieve the integrated fracturing and enhanced oil recovery for tight oil reservoirs, but also establishes a method to optimize the pumping schedule to maximize proppant concentration in the fracturing fluid without proppant-plugging risks during field operations based on laboratory measurements.

2. Materials and methods

2.1. Proppants and viscous slickwater

During hydraulic fracturing, proppants are pumped with the fracturing fluid that can keep hydraulic fractures open and accelerate hydrocarbon flow from the reservoir to the wellbore. In China, natural sands are typically used in the field to reduce the operation cost, especially in reservoirs shallower than 3500 m. Currently, 50/140 mesh sands are increasingly used that aims to support hydraulic fractures with different dimensions and further reduce the operation cost. In this study, 50/140 mesh sands are thus chosen to evaluate the proppant-carrying ability of the viscous slickwater. As shown in Fig. 1, over 98% of sands have diameters smaller than 230 μm, and the average diameter of the chosen sands is 190±42 μm.

Slickwater is typically a water solution of long-chain polymers, which can reduce over 75% of the flow friction of the fracturing fluid inside the wellbore during hydraulic fracturing. In this study, the conventional slickwater is prepared using a widely used anionic polyacrylamide as the friction reducer; the viscous slickwater is synthesized in the laboratory, which is a copolymer of acrylamide, acrylic acid, amino acid, and a few thousandths of organic amine (e.g., iminodiacetic acid) with hydrophobic groups for thickening through the hydrophobic association. In the viscous slickwater, diluted oil-in-water microemulsions are also used with a concentration of 0.1%; these microemulsions have an average particle size of 8 nm, and a thermodynamically stable structure that remains almost the same even after being sheared at 12,000 rpm for 15 min (Fig. 2). These diluted microemulsions (DME) can make the rock surface more water-wet and enhance the imbibition of the fracturing fluid (Liang et al., 2021); meanwhile, they can also enhance the intramolecular or intermolecular hydrophobic association or chelation among polymers that significantly enhances the viscosity of slickwater when the polymer concentration increases (i.e., viscous slickwater) (Yuan et al., 2023).

Importantly, tight reservoirs typically possess a large specific surface area, which leads to substantial adsorption losses of conventional surfactants. Prior studies have demonstrated that converting surfactants into thermodynamically stable nanodroplets can reduce adsorption loss by 1–2 orders of magnitude (Liang et al., 2021). Compared with the hydrophobic association induced by conventional surfactants, DME provides an additional “oil-core effect,” which further enhances hydrophobic association in hydrophobically modified polymers. The enhanced viscoelasticity and proppant-carrying performance observed in this study provide experimental verification of this mechanism.

2.2. Rheology test of viscous slickwater

Slickwater is typically a non-Newtonian fluid whose viscosity changes with the shear rate. This change is measured using a

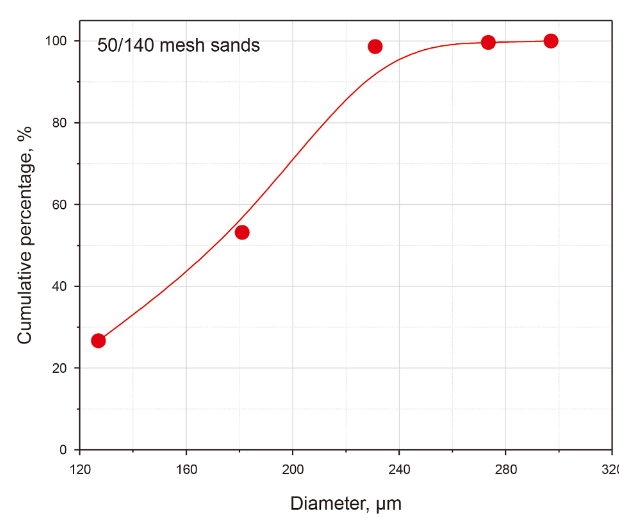

Fig. 1. Diameter distribution of proppants applied in this study (50/140 mesh natural sands).

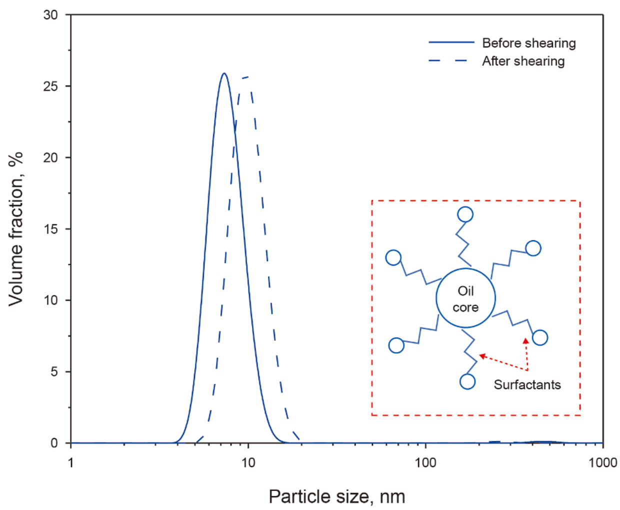

Fig. 2. Distribution of particle sizes of DME mixed with the viscous slickwater.

HAAKE rheometer (RheoStress-600) for both conventional slickwater and viscous slickwater chosen in this study, from which fitting parameters m and n can be obtained for characterizing the non-Newtonian fluid using the generalized power-law model as shown in Eq. (1).

$$\eta = m\dot{\gamma}^{n-1} \tag{1}$$

where η is the fluid viscosity, Pa·s; $\dot{\gamma}$ is the shear rate, s^{-1}; m and n are unitless fitting parameters.

Viscoelasticity is a crucial property that determines the proppant-carrying ability of the fracturing fluid under different flow conditions, and this is also characterized using the RheoStress 600 rheometer. After the fluid is added in the coaxial cylinder of the rheometer, a stress sweep is first conducted to find the linear viscoelastic region of the measured fluid, during which the shear stress increases from 0.001 to 20 Pa. Once the maximum stress of the linear viscoelastic region is obtained (about 0.05 Pa in this study), a frequency sweep is conducted at this selected stress with a stepped increasing frequency from 0.01 to 10 s^{-1} to obtain the change of storage and loss moduli of this viscoelastic fluid with shear rate.

2.3. Visualized proppant-carrying test in a rough fracture

In the laboratory, a transparent rough fracture model is built to visualize and evaluate the proppant-carrying ability of the fracturing fluid under different mimicked pumping conditions. The visualized rough fracture model is prepared by selecting a shale sample, fracturing it, and scanning the fracture surface. The surface roughness is quantified based on the scanning results (projected area:actual area = 0.36). To build this rough fracture model, a cubic outcrop sample with a side-length of 30 cm is first hydraulically fractured under a true triaxial condition that is analogues to the reservoir condition. The fractured sample is then 3D-scanned, 3D-printed, and triplicated using the transparent resin. Then, three pairs of these transparent resin samples are placed in a row to build a rough fracture model with a fracture length of 90 cm and a fracture width of 6 mm. The fracturing fluid and proppants are mixed in the upstream agitator tank, and pumped into the fracture model at a constant pumping rate, which is recorded by a downstream flowmeter as shown in Fig. 3. More details on building this visualized rough fracture model can refer to a previous published work (He et al., 2022).

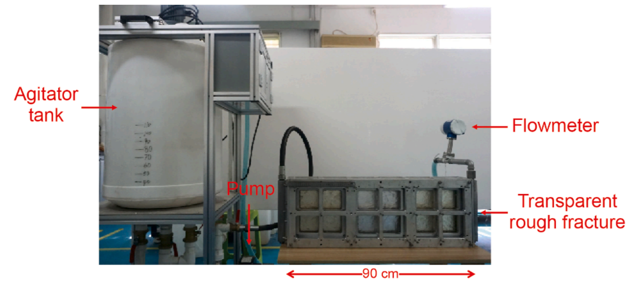

Fig. 3. Visualized rough fracture model for evaluating the proppant-carrying ability of the fracturing fluid.

When conducting the proppant-carrying test in the laboratory, the pumping rate of the slurry is designed according to the flow condition of proppants during hydraulic fracturing in the field by keeping the Reynolds number of particles a constant. For instance, assuming the reservoir thickness and fracture height are both 15 m, the dynamic fracture width is 8 mm during hydraulic fracturing, there are 3 clusters per stage and 1 double-wing fracture is generated per cluster, the pumping rate in the laboratory can be calculated as 0.03 m^3/min for a pumping rate of 12 m^3/min in the field, where the intra-fracture velocity of proppants is about 16.7 m/min (0.28 m/s) in this rough fracture model.

2.4. Evaluation of imbibition enhancement of DME-aided viscous slickwater in tight rocks

To evaluate the imbibition enhancement of the DME-aided viscous slickwater proposed in this study, the forced imbibition experiment with *in-situ* NMR scans and the pressure transmission experiment are both conducted; the former shows the change of water distribution with time in pores with different sizes, and the latter shows the change of pressure propagation rate during the shut-in treatment.

To conduct the forced imbibition experiment with *in-situ* NMR scans, relatively high-permeability reservoir rocks are chosen, which are obtained from the Chang-7 reservoir with permeabilities of around 0.1 mD. The core sample is first saturated and aged with the crude oil under 20 MPa for over a month; then, it is loaded in a core-holder with a confining pressure of 10 MPa, and placed in an NMR spectrometer (NIUMAG MacroMR12-150H-I). To minimize the NMR signal of hydrogen nuclei (^1H) in the aqueous phase, deuterium oxide (D_2O) is used to prepare the viscous slickwater that the change of NMR signals of the crude oil in different-sized pores can be observed during imbibition. The mimicked fracturing fluid with or without DME is injected into the core sample with a constant pressure-drop of 28 kPa across the sample (with a pressure gradient of about 0.56 MPa/m), which ensures a sufficient water supply from the upstream side of the sample for imbibition. During this imbibition experiment, the Car-Purcell-Meiboom-Gill (CPMG) sequence is applied to obtain the transverse relaxation time (T_2) of hydrogen nuclei in the crude oil. Since deuterium oxide does not have NMR signals, the reduction of T_2 signals in different-sized pores can show the water imbibition therein that substitutes the originally-saturated crude oil.

To conduct the pressure transmission experiment, relatively low-permeability reservoir rocks are chosen, which are obtained from the Jimusaer Basin with permeabilities of around 1 μD. The core sample is first wrapped with resin and sliced to a thickness of 1 cm, which is then saturated and aged in the crude oil at 20 MPa for over three months; after the sample is loaded in the pressure transmission cell, water with or without the DME solution is applied to the upstream of the sample with an initial pressure-drop of 0.6 MPa across the sample, during which both upstream and downstream pressures are recorded with time. More details on conducting the pressure transmission experiment can refer to a previous work (Liang et al., 2018).

3. Results and discussion

3.1. Rheology tests of viscous slickwater

Viscous slickwater is a non-Newtonian fluid that its viscosity changes with the shear rate. This change is measured using RheoStress-600 and then fitted with Eq. (1). As shown in Fig. 4, the viscosity of the slickwater decreases with the shear rate, and the fitting parameters m and n for the viscous slickwater with a concentration of 0.2% are 31.68 and 0.77, respectively. Since polymers of the viscous slickwater have hydrophobic groups for thickening and the added DME can also play as a "crosslinker", the viscosity of the viscous slickwater increases with the concentration. As shown in Fig. 5, the viscosity increases from 5 mPa·s (at a concentration of 0.1%) to 75 mPa·s (at a concentration of 0.8%), which can meet the requirement of continuously proppant-pumping during hydraulic fracturing in the field. When the brine with a salinity of 16,000 ppm is used to prepare the viscous slickwater, the fluid viscosity is significantly decreased and the increase in viscosity with the polymer concentration is also decreased as shown in Fig. 5. Since divalent cations (like Ca^{2+} or Mg^{2+}) in the brine can cause the agglomeration of polymer chains and shrink the size of single molecule, the reduced viscosity of the viscous slickwater in the brine indicates that the "crosslinking" effect of the chosen viscous slickwater is attributed to the intermolecular association among polymers. This "crosslinking" effect is reversible and likely causes less damage to propped fractures and the matrix than the conventional guar having the same viscosity. To overcome the impact of divalent cations to the viscous slickwater, cation-tolerant groups (like sulfonate groups) can be introduced into the polymer to substitute the original carboxylate groups; besides, nonionic or cationic polymers can be used to prepare the viscous slickwater. However, this is out of the scope of this work and can be outlines of a future study.

Viscoelasticity of the chosen viscous slickwater is characterized also by the RheoStress-600 rheometer using the frequency sweep

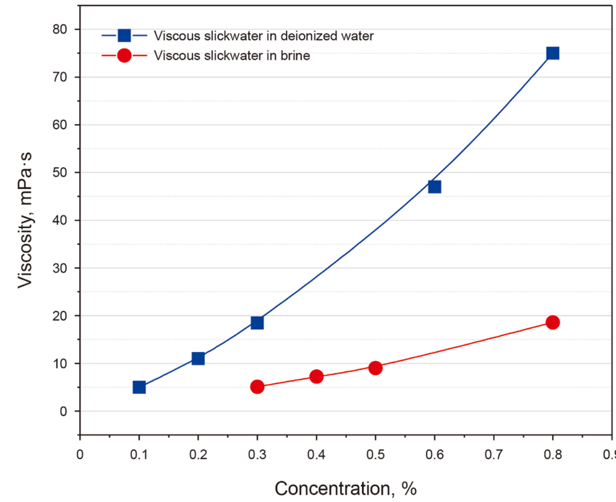

Fig. 5. Change of viscosity of the viscous slickwater with concentration in deionized water or brine.

mode. Fig. 6 shows changes of storage modulus (G') and loss modulus (G'') with the shear rate for the viscous slickwater at different polymer concentrations, and each pair of G' and G'' curves has an intersection point. On the left region of the intersection point where the shear force is small, the polymer behaves like a solid during shearing that the viscosity dominates the proppant-carrying performance; on the right region of the intersection point where the shear force is large, the polymer behaves like a liquid that the elastic energy released during polymer stretching can enhance the proppant-carrying performance of the fluid (Bai et al., 2021; Yuan et al., 2023). When the polymer concentration increases from 0.2% to 0.6% in the slickwater, the intersection points of G' and G'' curves shift from 1.30 to 0.01 Hz. Since the typical shear rate of fracturing fluid within main fractures is in the region of 0.1–10 Hz during hydraulic fracturing, the shift of the intersection point towards the lower shear-rate side not only indicates that the proppant-carrying ability of the viscous slickwater is dominated by the elasticity instead of the viscosity of the polymer, but also indicates that this dominance can extend to a wider range of pumping rate or fracture width when the polymer

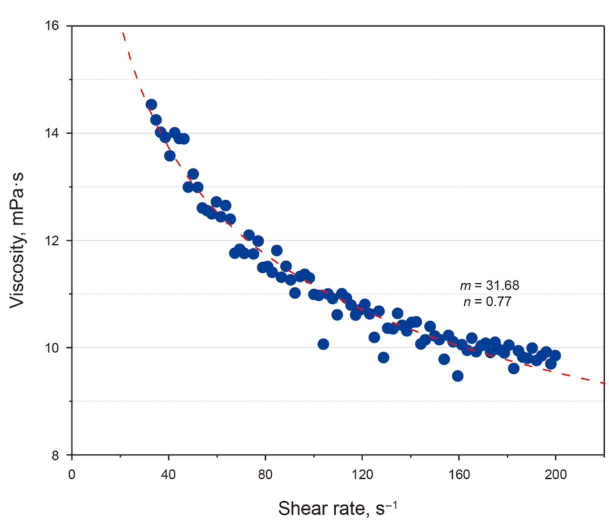

Fig. 4. Change of viscosity of the viscous slickwater (at a concentration of 0.2%) with shear rate.

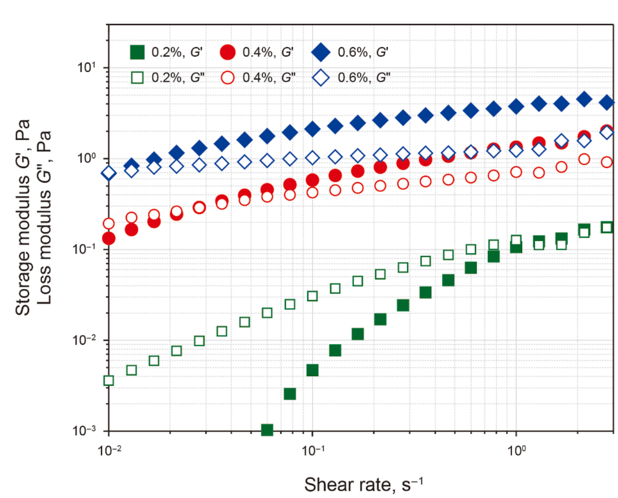

Fig. 6. Change of storage modulus (G') or loss modulus (G'') of the viscous slickwater with shear rate.

concentration increases in the fracturing fluid. More detailed calculations are shown in Section 3.3.

From the ratio of the storage modulus to the loss modulus, the relaxation time of this viscous slickwater can be calculated at each shear rate or angular frequency, as shown in Eq. (2); by further multiplying the relaxation time with the shear rate, the Weissenberg number (W_i) can be obtained as shown in Eq. (3). In Fig. 7, data points show the calculated W_i of the viscous slickwater from the measured storage and loss moduli (Fig. 6), from which curves are fitted using one type of power function to predict W_i at higher shear rates as ones of laboratory visualized proppant-carrying tests or slurry-flowing within hydraulic fractures during field operations; this is compared with the experimental data in Section 3.3.

$$\omega\lambda = \frac{G'(\omega)}{G''(\omega)} \tag{2}$$

where ω is the angular frequency; G' and G'' are storage and loss moduli as functions of angular frequency; λ is the relaxation time of the fluid.

$$W_i = \lambda\dot{\gamma} \tag{3}$$

where W_i is the Weissenberg number; and $\dot{\gamma}$ is the shear rate.

3.2. Visualized proppant-carrying tests in a rough fracture

The transparent rough fracture model is used to evaluate the proppant-carrying ability of the viscous slickwater at different mimicked fracturing conditions. In each experiment, 50/140 mesh natural sands are mixed with 0.2% viscous slickwater in the upstream agitator tank, and then pumped into the fracture model at a constant pumping rate; the experiment is repeated for different sand concentrations changing from 10% to 30%, and different intra-fracture velocities of slurry changing from 3.8 to 29 m/min. Fig. 8 shows the slurry flowing through the transparent rough fracture model at a sand concentration of 20% and an intra-fracture velocity of 12.5 m/min; at this flow condition, sands uniformly distribute in the flowing slurry and the settling of sands is barely observed. When the sand concentration increases to 30%, 0.2% viscous slickwater is unable to carry sands without settling at this flow condition; sands gradually settle to the bottom of the fracture and form a sand-bank as can be seen in Fig. 9. Experimental results of sand settling at different flow conditions are depicted in Fig. 10, from which the minimal pumping rate of the viscous slickwater to prevent the sand settling (sand plugging) can be estimated for designing field operations. Assuming that each stage has 3 main fractures with fracture heights of 15 m and fracture widths of 8 mm, the minimal pumping rate to continuously carry 30% sands with 0.2% viscous slickwater is about 14 m^3/min during hydraulic fracturing in the field, which is equivalent of an intra-fracture velocity of about 20 m/min.

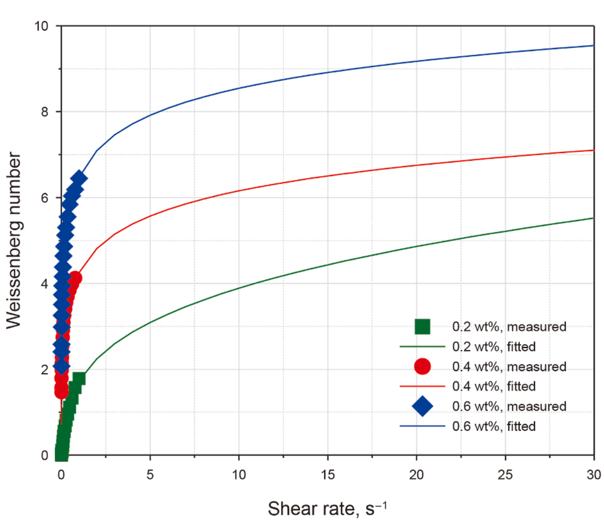

Fig. 7. Calculated Weissenberg number and fitted curves of the viscous slickwater with different polymer concentrations.

Besides the flow experiment, the transparent rough fracture model can be also used to measure the settling rate of proppants in the viscous slickwater without a horizonal velocity. To conduct this test, 50/140 mesh natural sands are mixed with the viscous slickwater in the upstream agitator tank at a predetermined concentration, and then pumped into the transparent fracture model at a constant pumping rate that sands do not settle; once the fracture model is uniformly filled with the slurry, the pump is turned off to allow sands to settle. From both of the captured settling sands and the growth of sand-bank at the fracture bottom, the average settling rate of sands in this type of fracturing fluid can be obtained. Fig. 11 shows data points and the corrected Stokes' equation from a previous published work that uses the same rough fracture model while considering the impacts of proppant diameter and concentration on the settling rate of sands (He et al., 2022). The red data point shows the measured settling rate of 50/140 mesh sands at a concentration of 20% in 0.2% viscous slickwater in this study; the settling rate is 0.7±0.3 cm/s, which matches well with the previously-proposed settling model as shown as the magenta dash curve in Fig. 11. This good match indicates that the proppant-carrying ability of the viscous slickwater is determined by the fluid viscosity at the low shear-rate region or when the pumping is finished; meanwhile, this further confirms that the proppant-carrying ability of the viscous slickwater during the pumping is determined by fluid elasticity instead of fluid viscosity as previously discussed.

3.3. Shear rate calculation and proppant-carrying by viscoelasticity

Viscous slickwater is a non-Newtonian fluid whose viscosity changes with the shear rate. Therefore, the Stokes' equation, which assumes a constant fluid viscosity, cannot accurately predict the proppant-carrying ability of the viscoelastic fluid during hydraulic fracturing. Considering the change of fluid viscosity with the shear rate as described by Eq. (1), the horizontal velocity of the fluid flowing in a vertical fracture can be described by Eq. (4) (Bird et al., 2006). Integrating this velocity over the entire fracture width (from $x = -B$ to $x = B$) gives the volumetric flow rate of the fluid in this vertical fracture, as shown in Eq. (5).

$$V_y = \left[\frac{(P_0 - P_L)B}{mL}\right]^{\frac{1}{n}} \frac{B}{1+\frac{1}{n}} \left[1 - \left(\frac{x}{B}\right)^{1+\frac{1}{n}}\right] \quad 0 \le x \le B \tag{4}$$

$$Q_y = 2H\left[\frac{(P_0 - P_L)B}{mL}\right]^{\frac{1}{n}} \frac{B}{1+\frac{1}{n}} \left(B - \left(\frac{B}{2+\frac{1}{n}}\right)\right) \tag{5}$$

where V_y is the fluid velocity along the direction of fracture length (y), m/s; Q_y is the volumetric flow rate of the fluid through the fracture, m^3/s; P_0 is the pressure at the fracture inlet ($y = 0$), Pa; P_L is the pressure at the fracture outlet ($y = L$), Pa; L is the fracture length, m; B is half the fracture width, m; H is the fracture height,

Fig. 8. Slurry flows in the transparent rough fracture model without settling (0.2% viscous slickwater, 20% sands, and an intra-fracture velocity of 12.5 m/min).

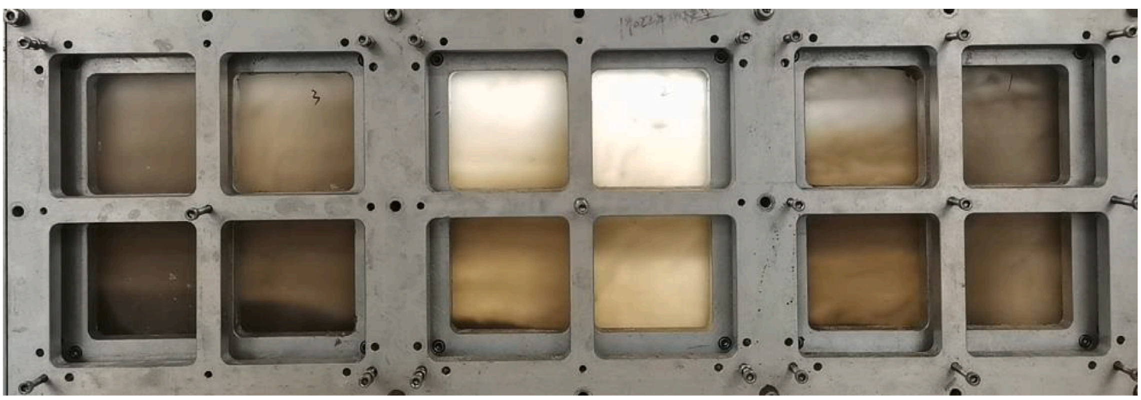

Fig. 9. Slurry flows in the transparent rough fracture model with settling (0.2% viscous slickwater, 30% sands, and an intra-fracture velocity of 12.5 m/min).

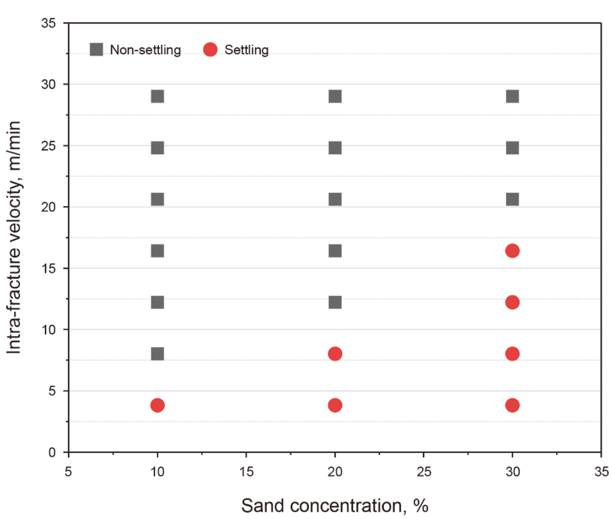

Fig. 10. Flow conditions of the slurry with or without sand-settling (0.2% viscous slickwater).

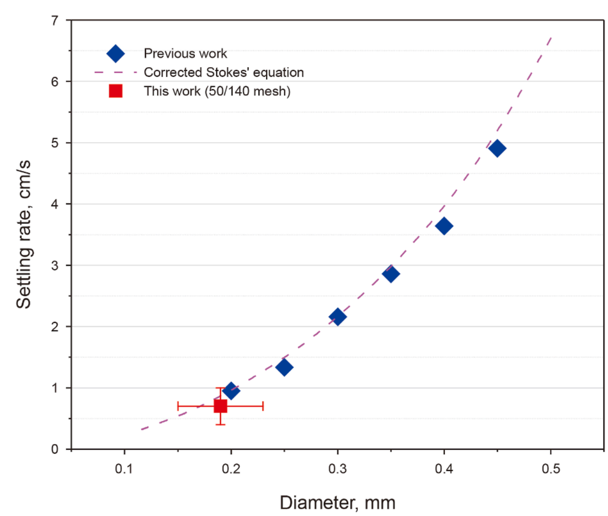

Fig. 11. Comparison between the measured settling rate of sands in this work and the corrected Stokes' equation proposed by the previous work (slickwater viscosity = 10 mPa·s).

m; x is the distance in the direction of fracture width (x), where the zero point locates at the center of fracture width, m; m and n are unitless fitting parameters as shown in Eq. (1).

Combining Eqs. (4) and (5) by eliminating the pressure gradient term gives the distribution of the horizontal velocity of the fluid along the fracture width, as shown in Eq. (6). By further taking the derivative in the direction of fracture width (x), the distribution of the shear rate of the flowing fluid in the fracture can be obtained as shown in Eq. (7), where the maximum shear rate occurs at the fracture face ($x = \pm B$).

$$V_y = \frac{Q}{2H} \frac{\left(\frac{1}{n}\right)+1}{B\left(1-\left(\frac{1}{2+\frac{1}{n}}\right)\right)} \frac{1}{1+\frac{1}{n}} \left[1-\left(\frac{x}{B}\right)^{1+\frac{1}{n}}\right] \tag{6}$$

$$\frac{\mathrm{d}V_y}{\mathrm{d}x} = \frac{Q}{2H} \frac{1}{B\left(1-\left(\frac{1}{2+\frac{1}{n}}\right)\right)} \left[-\frac{1}{B}\left(1+\frac{1}{n}\right)\left(\frac{x}{B}\right)^{\frac{1}{n}}\right] \tag{7}$$

At the field scale, the pumping rate is 13 m^3/min with three perforation clusters, a fracture height of 30 m, and a fracture width of 6 mm. Under these conditions, the average fluid velocity inside the fracture is calculated to be 12.22 m/min. Considering that the central region of the fracture is the main zone for proppant transport, the shear rate is evaluated at a position 1.5 mm away from the fracture wall based on the 6 mm fracture model. When the polymer concentrations are 0.2, 0.4, and 0.6 wt%, the corresponding shear rates within the fracture are 85.6, 52.1, and 23.9 s^{-1}, respectively. Based on the selected field parameters in this study, the maximum shear rate within the fracture is estimated to be no greater than 86 s^{-1}.

Then, the proppant-carrying results of viscous slickwater with different polymer concentrations (0.2, 0.4, and 0.6 wt%) in the visualized rough-fracture model are calculated and compared in Fig. 12, all under a fixed 10% sand concentration. In Fig. 12, the flow rate of each case is converted to the shear rate using Eq. (7), and the viscoelasticity at each shear-rate condition is converted to the Weissenberg number (W_i) using Eqs. (2) and (3). Cases without obvious sand settling are shown as hollow symbols, whereas those with clear sand-bank formation are shown as solid symbols.

By combining the rheological measurements with the calculated shear rates within a fracture, this study demonstrates that the Weissenberg number can quantitatively determine the proppant-carrying threshold of the fracturing fluid. Because Weissenberg number inherently reflects the level of elasticity, we further compared fluids with different viscosities and found that their proppant-carrying thresholds converge to essentially the same Weissenberg number when transporting the same proppant concentration. Therefore, Weissenberg number serves as a reliable indicator for predicting the proppant-carrying threshold under given fracturing conditions. Comparing all cases reveals that the viscous slickwater with three different polymer concentrations have the same proppant carrying threshold when scaled by the Weissenberg number, measured at 4.7 for cases with 10% sand concentration. This observation indicates that the Weissenberg number can quantify the proppant-carrying capacity of a viscoelastic fluid at specific proppant and polymer concentrations under a given hydraulic fracturing flow condition. Nevertheless, further experimental validation is needed across a broader range of proppant concentrations and shear rates. Field validation requires testing the proppant-carrying threshold under a wider range of pumping rates with different polymer and sand concentrations. In addition, each test condition must be maintained for a sufficient time to allow the slurry to reach the reservoir before the threshold can be evaluated.

To elucidate the influence of elasticity on proppant-carrying performance, two slickwater fluids with identical viscosity but different viscoelasticity are prepared and evaluated using a fracture-flow test. The viscoelasticity of the slickwater is adjusted through salinity modification, which effectively weakens the hydrophobic association while keeping the same apparent viscosity of both samples at approximately 9 mPa·s.

The difference in viscoelasticity between the two fluids are shown in Fig. 13, and their proppant-carrying performances in the fracture-flow test are presented in Figs. 14 and 15. The slickwater with lower viscoelasticity develops a clear sand bank, with its corresponding Weissenberg number of below 4.7 (see Fig. 14). In contrast, the slickwater with higher viscoelasticity shows no sand-bank formation, and its Weissenberg number exceeds 4.7 (Fig. 15).

3.4. Imbibition enhancement through wettability alteration in tight rocks

In the viscous slickwater, the diluted microemulsion (DME) is added to enhance the intramolecular or intermolecular hydrophobic association among polymers that can play a similar role as the "crosslinker" to enhance the fluid viscosity. Following the breakdown and/or degradation of polymers after hydraulic fracturing, DME can make the oil-wet rock water-wet and trigger the spontaneous imbibition to enhance oil recovery (Liang et al.,

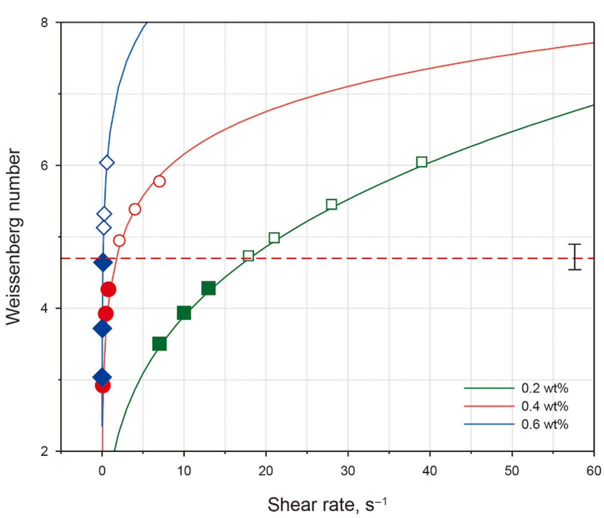

Fig. 12. Flow conditions of the slurry (in Weissenberg numbers) in the transparent rough fracture model with (hollow data points) or without (solid data points) sand-settling in the viscous slickwater with different polymer concentrations.

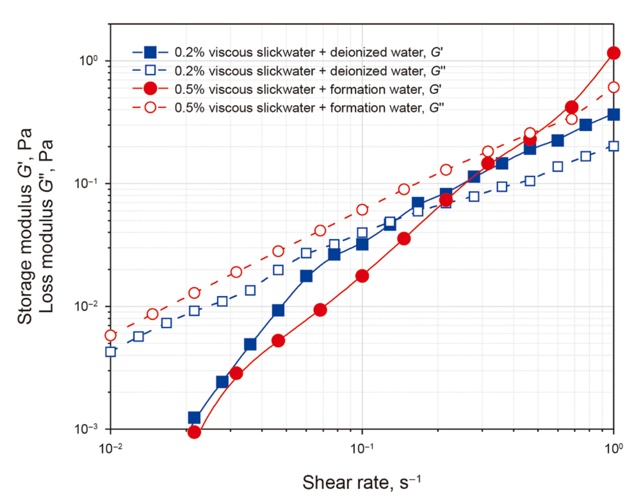

Fig. 13. Comparison of storage and loss moduli between 0.2% viscous slickwater in the deionized water and 0.5% viscous slickwater in the formation brine (which have the same viscosity).

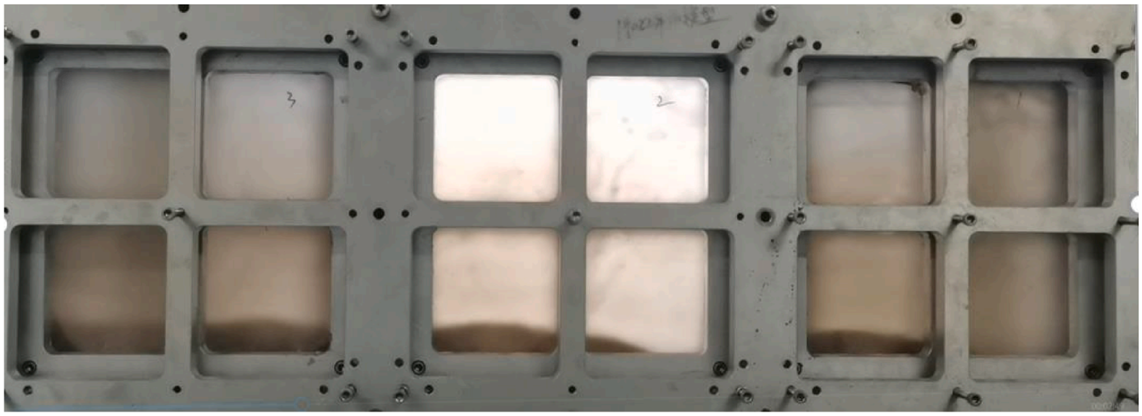

Fig. 14. Slurry flows in the transparent rough fracture model with settling (0.5% viscous slickwater in the formation brine, 10% sands, and an intra-fracture velocity of 8 m/min).

Fig. 15. Slurry flows in the transparent rough fracture model with settling (0.2% viscous slickwater in the deionized water, 10% sands, and an intra-fracture velocity of 8 m/min).

2021). For relatively high permeability reservoir rocks obtained from the Chang-7 reservoir (around 0.1 mD), water imbibition in different-sized pores can be directly observed using the *in-situ* NMR scans. Fig. 16 shows the change of T_2 signal during water imbibition with or without using DME. For the crude-oil-saturated rock, a two-peak spectrum is observed, the area below which gives a base value of the initial oil saturation. When D_2O (i.e., a type of water without ^1H resonance) is cycling at the rock upstream with a pressure gradient of 0.56 MPa/m across the rock length, the strength of T_2 signals slightly decreases with time since the crude oil is displaced by the T_2-signal-free D_2O (Fig. 16(a)). For an oil-wet rock sample where the spontaneous imbibition is hindered, only a small amount of water can enter the rock to displace the crude oil therein, and the oil recovery rate is less than 10% after 20 d of the

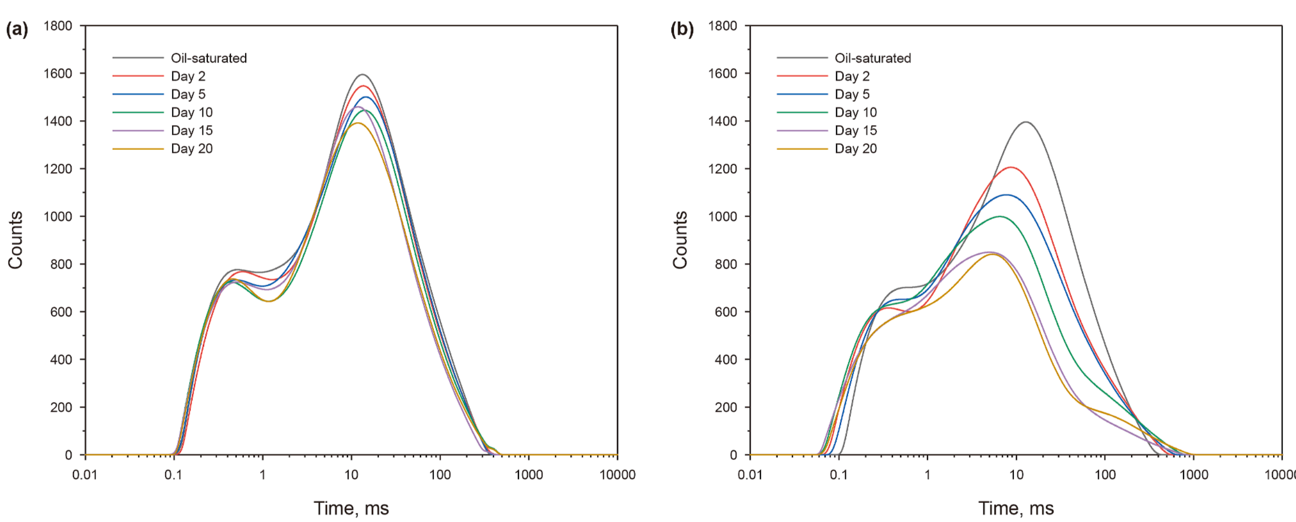

Fig. 16. Change of T_2 spectrum during forced imbibition without (**a**) or with (**b**) DME in the mimicked fracturing fluid.

experiment. When the DME solution is used that the shale sample is altered to water-wet, the strength of T_2 signals decreases obviously with time, especially in large pores whose relaxation times are longer than 1 ms (Fig. 16(b)). This observation also agrees with previous experimental results that water imbibition starts from relatively large pores after wettability alteration (Zhou et al., 2019; Liang et al., 2021; Zhao et al., 2021). The oil recovery rate increases up to 35% after 20 d of the experiment when the DME solution is used.

For relatively low permeability reservoir rocks obtained from the Jimusaer Basin (around 1 μD), the conventional coreflood is time-consuming and low in accuracy. Therefore, the pressure transmission experiment is conducted to evaluate the enhancement of oil recovery when wettability alteration is triggered. After the shale sample is saturated and aged in the crude oil for over three months, the pressure transmission experiment is conducted first with the crude oil to measure the rock permeability, which gives 1.6 μD for the shale sample used in this study. Then, an upstream pressure of 0.6 MPa is applied by water, which gives an initial pressure gradient of 60 MPa/m for the pressure transmission experiment. As shown in Fig. 17, pressure starts to propagate from the upstream to the downstream, and the equilibrium cannot be achieved even after 1000 min of the experiment. When this pressure transmission experiment is repeated in a similar shale sample using the DME solution, the pressure propagation is significantly accelerated by two orders of magnitude, and the pressure equilibrium is achieved after 30 min of the experiment. After wettability alteration occurs, the imbibition rate of water reaches 0.025 cm/min in this case.

4. Field test and application

After laboratory evaluations are completed for the chosen viscous slickwater, a field test is conducted to evaluate the applicability of the threshold chart of the intra-fracture velocity to prevent proppant settling and plugging. In this field test, a vertical exploration well is chosen in the Chang-7 Formation, where 9 layers of thin reservoirs are exploited together with a total thickness of about 47 m; in each thin layer, 1 or 2 m height is perforated with a phase angle of 60° and a perforation density of 16 holes per meter, which gives a total perforation height of 10 m (160 perforation holes in total) across the entire 9 layers of the reservoir. During hydraulic fracturing, 0.2% viscous slickwater is pumped into the well with a constant pumping rate of 10 m^3/min, and three stages of proppant-carrying test are conducted in sequence, where the sand concentration steps up to 25% (400 kg/m^3) in the first two stages and up to 40% (637 kg/m^3) in the last stage. A total volume of 30 m^3 sands is pumped in each stage, and 100 kg of diverters are pumped between every two stages to increase the coverage of the generated fracture network.

The change of wellhead pressure during this three-stage field test is shown in Fig. 18. In the first testing stage, no sand plugging is observed and the wellhead pressure slightly increases from 17 to 19 MPa, which can attribute to the density change of the slurry in the wellbore. As shown in the threshold chart (Fig. 10), the minimal intra-fracture velocity to prevent the sand settling is 12 m/min for 0.2% viscous slickwater with a sand concentration of 25%. Considering that the fracture height is likely 20–45 m and the fracture width is 10 mm, the intra-fracture velocity of 12 m/min can range from 5 to 10 m^3/min for the testing well, which is lower than the pumping rate applied in hydraulic fracturing. Therefore, no sand plugging observed in the first stage of the field test agrees with the threshold chart (Figs. 10 and 12) obtained from the laboratory proppant-carrying tests using the visualized rough fracture model.

After the first stage, a diversion treatment is conducted, which is followed by another 30 m^3 of sands being pumped in the same manner as the first stage. However, in this second stage, the wellhead pressure increases rapidly from 15 to 23 MPa when the slug of slurry with a sand concentration of 22% reaches the bottom-hole (at about 76 min). For a vertical well in a formation where the difference of two horizontal stresses is large (like Chang-7 in this test), although new fractures can be generated after the diversion treatment, they change directions quickly and merge to initial fractures along the direction of the maximum horizontal stress ($S_{h,max}$) (Wang et al., 2019, 2020a). When this happens, the initial propped fractures can inhibit the sand migration during the second stage; therefore, the sand plugging is observed even when the intra-fracture velocity is still above the threshold of 12 m/min in this second stage (in 80–90 min).

After the second testing stage followed by the second round of diversion treatment, the third testing stage is conducted where the viscous slickwater concentration is increased up to 0.6% and the sand concentration steps up to 40% (about 630 kg/m^3). As shown in Fig. 18, the wellhead pressure decreases normally with the increase in the slurry density at the beginning of pumping; however, after 11 m^3 of sands is pumped and the slurry with a sand

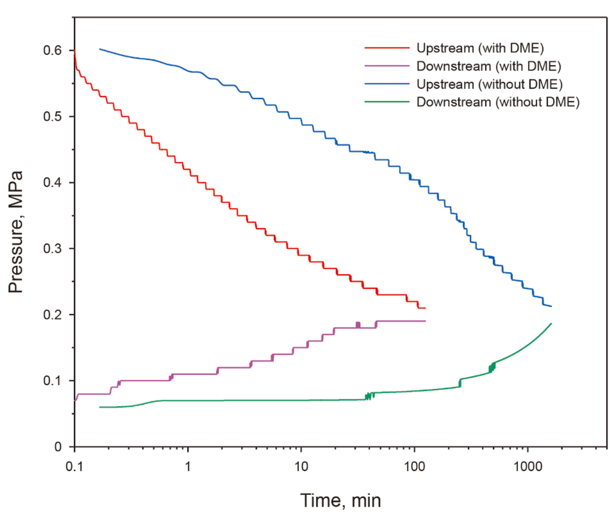

Fig. 17. Change of upstream and downstream pressures during pressure transmission tests with or without DME in the mimicked fracturing fluid.

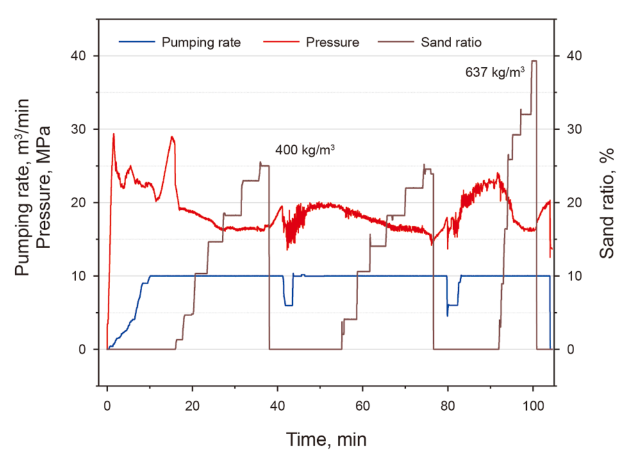

Fig. 18. Proppant-carrying ability of the viscous slickwater in a vertical exploration well in a shale reservoir.

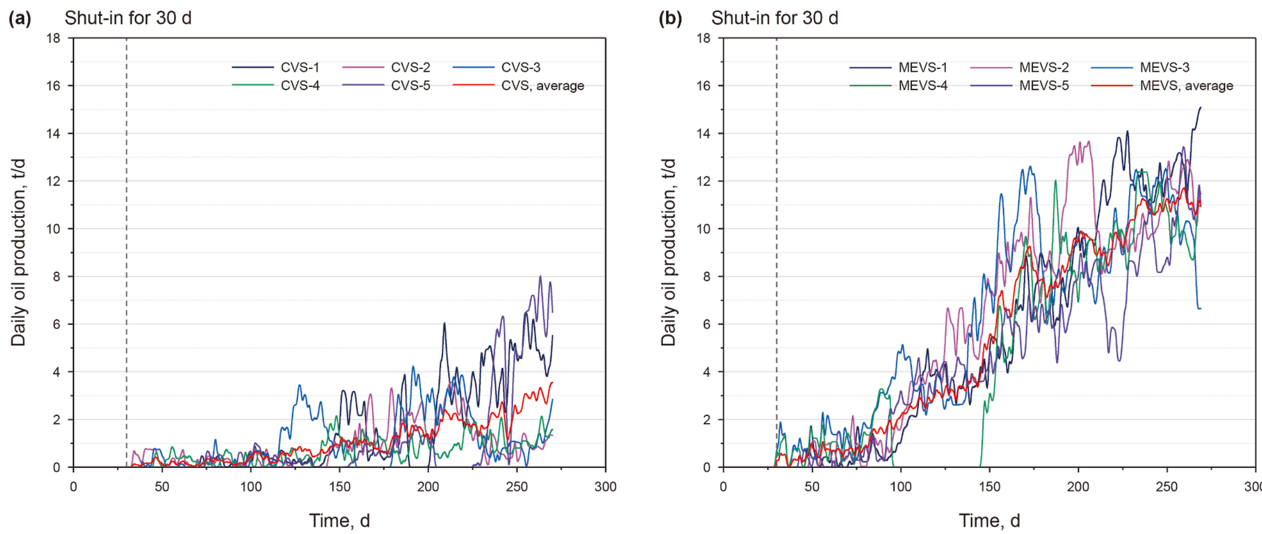

Fig. 19. Production comparison between wells using the conventional viscous slickwater (CVS) (**a**) and the DME-aided viscous slickwater (MEVS) (**b**).

concentration of 30% reaches the bottom-hole, the wellhead pressure starts to increase rapidly (at about 101 min). The timing of the pressure increase and the increasing rate of the pressure are both similar to those in the second stage; besides, in laboratory proppant-carrying tests, no sand settling is observed when testing 0.6% viscous slickwater with a wide range of intra-fracture velocities and sand concentrations. Therefore, the sand plugging observed in the third testing stage is likely also due to the merge of diverted fractures with previously-generated ones, which inhibits the migration of the following pumped sands.

After the proppant-carrying ability of the viscous slickwater is examined in a vertical well in the Chang-7 Formation, two types of viscous slickwater are further compared in two neighboring pads for their potentials in enhanced oil recovery. Two pads are about 2 km apart, and wells on both pads are drilled to develop the same Chang-7 Formation. Permeability of the formation rock ranges from 0.08 to 0.17 mD, porosity from 7% to 11%, oil saturation from 53% to 65%, and the minimum horizontal stress ranges from 28.0 to 32.0 MPa. A conventional viscous slickwater that is commercially available in used in 5 horizontal wells on one platform, while MEVS developed in this study is used in 5 horizontal wells on the other platform. All wells have lengths of around 1500 m and 4–6 clusters per stage with one diversion treatment in between; during hydraulic fracturing, 140–180 m^3 sands are pumped into the well per stage with a constant pumping rate of 10 m^3/min as in the proppant-carrying field test. After hydraulic fracturing, all wells are shut in for 30 d and then opened for production. The production histories of ten wells in two pads are compared in Fig. 19, where the average daily oil production rate of conventional viscous slickwater wells is about 3.4 t/d while that of MEVS wells is about 11.2 t/d after 270 d of production. This threefold enhancement of oil production in the field agrees well with laboratory results that DME can enhance the imbibition of the fracturing fluid and mobilize the oil in pores of tight rocks.

In general, except for the influence of diversion treatment, the field fracturing test agree well with the laboratory evaluations that the chosen viscous slickwater has a promising proppant-carrying ability at low (0.2%) to high (0.6%) concentrations, and it can ensure continuous sand-pumping up to a sand concentration of over 400 kg/m^3 at a pumping rate of 10 m^3/min. Adding DME in the viscous slickwater not only can enhance the proppant-carrying ability of the fluid by enhancing the intramolecular or intermolecular hydrophobic association among polymers, but also can enhance the imbibition of the fluid that mobilizes the crude oil in place and enhances the oil recovery rate. Because of its excellent proppant-carrying performance, the viscous slickwater allows for higher sand concentrations to be pumped, which leads to a 31% reduction in water usage at an equivalent proppant intensity per lateral length. In addition, the improved forced imbibition facilitates a 2.3-fold enhancement in oil production without additional costs.

5. Conclusions

Economically recovering oil from tight or shale oil reservoirs requires both an extensively developed propped fracture network and a rock matrix with sufficient oil mobility. This imposes higher demands on the fracturing fluid. In this study, a DME-aided viscous slickwater (MEVS) is developed in the laboratory, where DME can enhance the viscoelasticity of the slickwater through hydrophobic association during hydraulic fracturing while preventing surfactant adsorption to increase the depth of wettability alteration after hydraulic fracturing. The former characteristic enhances the proppant-carrying ability of the slickwater without obviously increasing the fluid viscosity, which ensures the formation of an extensively developed and propped fracture network; the latter characteristic enlarges the area of rock matrix being altered to water-wet, which enhances oil recovery through both water imbibition and increased oil relative permeability. Meanwhile, laboratory evaluation is established to elucidate the mechanism of this MEVS to ensure its successful application in the field, as summarized below.

(1) A visualized rough fracture model is developed to evaluate the proppant-carrying ability of the fracturing fluid at a similar flow condition as hydraulic fracturing in the field. Results show that increasing the elasticity can significantly improve the proppant-carrying ability of the fluid without increasing the fluid viscosity, which combines advantages of conventional slickwater water and crosslinked gel.
(2) The inner-fracture shear rate is derived for the power-law non-Newtonian fluid, from which the Weissenberg number is calculated to quantify the viscoelasticity of the viscous slickwater for carrying proppants. Comparing with results

from visualized proppant-carrying tests within the rough fracture, a threshold of Weissenberg number has been proposed that can be used to quantitatively characterize the proppant-carrying ability of the viscous slickwater at certain proppant and polymer concentrations during hydraulic fracturing.

(3) After the propped fracture network is generated, DME is released to enhance oil recovery through wettability alteration. The *in-situ* NMR T_2 results show that oil is recovered from large pores to small pores, and the recovery rate can increase up to 35% after 20 d of imbibition. The pressure transmission experiment shows that the pressure propagation can be significantly accelerated by two orders of magnitude comparing to the case without using any surfactant.

Field tests are successfully accomplished. During hydraulic fracturing, 0.2% viscous slickwater can continuously carry 400 kg/m^3 sands at a pumping rate of 10 m^3/min without potential sand plugging issues, which agrees with the threshold chart obtained from the laboratory proppant-carrying tests using the visualized rough fracture model. After hydraulic fracturing, the average daily oil production rate of wells using the MEVS increases up to threefold of wells using the conventional viscous slickwater, which also agrees with laboratory observations that DME can enhance the imbibition of the fracturing fluid and mobilize oil from small pores of tight rocks.

This work not only proposes an avenue to achieve the integrated fracturing and enhanced oil recovery for tight oil reservoirs, but also establishes a method to optimize the pumping schedule to maximize proppant concentration in the fracturing fluid without proppant-plugging risks during field operations based on laboratory measurements.

CRediT authorship contribution statement

Tian-Bo Liang: Writing – review & editing, Writing – original draft, Supervision, Funding acquisition. **Jun-Lin Wu:** Writing – original draft, Investigation, Data curation. **Zi-Lin Deng:** Investigation, Data curation. **Shuai Yuan:** Investigation, Data curation. **Hao Liu:** Investigation, Data curation. **Bin Wang:** Investigation. **Fu-Jian Zhou:** Supervision, Funding acquisition.

Declaration of competing interest

The authors declare that they have no known competing financial interests or personal relationships that could have appeared to influence the work reported in this paper.

Acknowledgements

This work is financially supported by the General Program Grant from the National Natural Science Foundation of China (52274051 and 52174045), the Foundation for Innovative Research Groups of the National Natural Science Foundation of China (51521063), and the National Science and Technology Major Project (2025ZD1405401).

References

Anschutz, D.A., Lowrey, T.A., Stribling, M., Wildt, P.J., 2019. An in-depth study of proppant transport and placement with various fracturing fluids. In: SPE Annual Technical Conference and Exhibition. https://doi.org/10.2118/196073-MS.

Ba Geri, M., Ellafi, A., Flori, R., Noles, J., Kim, S., 2019a. Viscoelastic characterization effect of high-viscosity friction reducers and proppant transport performance in high-TDS environment. In: SPE Annual Technical Conference and Exhibition. https://doi.org/10.2118/196014-MS.

Ba Geri, M., Imqam, A., Bogdan, A., Shen, L., 2019b. Investigate the rheological behavior of high viscosity friction reducer fracture fluid and its impact on proppant static settling velocity. In: SPE Oklahoma City Oil and Gas Symposium. https://doi.org/10.2118/195227-MS.

Ba Geri, M., Imqam, A., Flori, R., 2019c. A critical review of using high viscosity friction reducers as fracturing fluids for hydraulic fracturing applications. In: SPE Oklahoma City Oil and Gas Symposium. https://doi.org/10.2118/195191-MS.

Bai, H., Zhou, F., Zhang, M., Gao, X., Xu, H., Yao, E., Wang, J., Li, Y., 2021. Optimization and friction reduction study of a new type of viscoelastic slickwater system. J. Mol. Liq. 344, 117876. https://doi.org/10.1016/j.molliq.2021.117876.

Barati, R., Liang, J.-T., 2014. A review of fracturing fluid systems used for hydraulic fracturing of oil and gas wells. J. Appl. Polym. Sci. 131 (16). https://doi.org/10.1002/app.40735.

Beason, R., Fagan, J., 1995. The determination of dynamic proppant concentration field in slot flow in the FFCF. In: SPE Annual Technical Conference and Exhibition. https://doi.org/10.2118/30515-MS.

Biheri, G., Imqam, A., 2022. Proppant transport using high-viscosity friction reducer fracture fluids at high-temperature environment. SPE J. 27, 60–76. https://doi.org/10.2118/206750-PA.

Bird, R.B., Stewart, W.E., Lightfoot, E.N., 2006. In: Transport Phenomena, Revised second ed. Wiley.

Blyton, C.A., Gala, D.P., Sharma, M.M., 2018. A study of proppant transport with fluid flow in a hydraulic fracture. SPE Drill. Complet. 33, 307–323. https://doi.org/10.2118/174973-PA.

Gale, J.F.W., Elliott, S.J., Rysak, B.G., Ginn, C.L., Zhang, N., Myers, R.D., Laubach, S.E., 2021. Fracture description of the HFTS-2 slant core, Delaware Basin, West Texas. In: SPE/AAPG/SEG Unconventional Resources Technology Conference. https://doi.org/10.15530/urtec-2021-5175.

Gomaa, A.M., Gupta, D.V.S., Carman, P., 2015a. Viscoelastic behavior and proppant transport properties of a new high-temperature viscoelastic surfactant-based fracturing fluid. In: SPE International Symposium on Oilfield Chemistry. https://doi.org/10.2118/173745-MS.

Gomaa, A.M., Gupta, D.V.S., Carman, P.S., 2015b. Proppant transport? Viscosity is not all it's cracked up to be. In: SPE Hydraulic Fracturing Technology Conference. https://doi.org/10.2118/173323-MS.

He, X., Wei, D., Yu, H., Bai, B., Chen, A., Liang, T., 2022. Proppant migration within a rough hydraulic fracture. J. Porous Media 26 (4). https://doi.org/10.1615/JPorMedia.2022043344.

Hu, X., Wu, K., Song, X., Yu, W., Zuo, L., Li, G., Shen, Z., 2018. Development of a new mathematical model to quantitatively evaluate equilibrium height of proppant bed in hydraulic fractures for slickwater treatment. SPE J. 23, 2158–2174. https://doi.org/10.2118/191360-PA.

Hu, Y.T., Chung, H., Maxey, J.E., 2015a. What is more important for proppant transport, viscosity or elasticity?. In: SPE Hydraulic Fracturing Technology Conference https://doi.org/10.2118/173339-MS.

Hu, Y.T., Kishore, T., Maxey, J., Loveless, D., 2015b. Effects of crosslinking chemistry on proppant suspension in guar networks. In: SPE International Symposium on Oilfield Chemistry. https://doi.org/10.2118/173726-MS.

Hu, Y.T., Larsen, T., Martysevich, V., 2015c. Study of proppant suspending using a multipass slot flow apparatus. In: SPE Production and Operations Symposium. https://doi.org/10.2118/173629-MS.

Lei, Q., Xu, Y., Cai, B., Guan, B., Wang, X., Bi, G., Li, H., Li, S., Ding, B., Fu, H., Tong, Z., Li, T., Zhang, H., 2022. Progress and prospects of horizontal well fracturing technology for shale oil and gas reservoirs. Petrol. Explor. Dev. 49, 191–199. https://doi.org/10.1016/S1876-3804(22)60015-6.

Lei, Q., Weng, D., Guan, B., Shi, J., Cai, B., He, C., Sun, Q., Huang, R., 2023. Shale oil and gas exploitation in China: Technical comparison with US and development suggestions. Petrol. Explor. Dev. 50, 1–8. https://doi.org/10.11698/PED.2022.0714.

Li, N., Jin, Z., Wang, H., Zou, Y., Zhang, S., Li, F., Zhou, T., Jiang, M., 2023. Investigation into shale softening induced by water/CO_2-rock interaction. Int. J. Rock Mech. Min. Sci. 161, 105299. https://doi.org/10.1016/j.ijrmms.2022.105299.

Liang, T., Luo, X., Nguyen, Q., DiCarlo, D.A., 2018. Computed-tomography measurements of water block in low-permeability rocks: Scaling and remedying production impairment. SPE J. 23, 762–771. https://doi.org/10.2118/189445-PA.

Liang, T., Zhao, X., Yuan, S., Zhu, J., Liang, X., Li, X., Zhou, F., 2021. Surfactant-EOR in tight oil reservoirs: Current status and a systematic surfactant screening method with field experiments. J. Pet. Sci. Eng. 196, 108097. https://doi.org/10.1016/j.petrol.2020.108097.

Longoria, R.A., Liang, T., Huynh, U.T., Nguyen, Q.P., DiCarlo, D.A., 2017. Water blocks in tight formations: The role of matrix/fracture interaction in hydrocarbon-permeability reduction and its implications in the use of enhanced oil recovery techniques. SPE J. 22, 1393–1401. https://doi.org/10.2118/185962-PA.

Malhotra, S., Sharma, M.M., 2011. A general correlation for proppant settling in VES fluids. In: SPE Hydraulic Fracturing Technology Conference. https://doi.org/10.2118/139581-MS.

Malhotra, S., Lehman, E.R., Sharma, M.M., 2014. Proppant placement using alternate-slug fracturing. SPE J. 19, 974–985. https://doi.org/10.2118/163851-PA.

Ouyang, L., Yango, T., Zhu, D., Hill, A.D., 2012. Theoretical and experimental modeling of residual gel filter-cake displacement in propped fractures. SPE Prod. Oper. 27, 363–370. https://doi.org/10.2118/147692-PA.

Poole, R., 2012. The Deborah and Weissenberg numbers. Rheol. Bull. 53 (2), 32–39.
Poppel, B., 2020. Fighting the fear: Overcoming preconceived notions of low polymer cross-linked gels and high viscosity polyacrylamides in unconventional fracturing. In: SPE Hydraulic Fracturing Technology Conference and Exhibition. https://doi.org/10.2118/199760-MS.
Raterman, K.T., Farrell, H.E., Mora, O.S., Janssen, A.L., Gomez, G.A., Busetti, S., McEwen, J., Davidson, M., Friehauf, K., Rutherford, J., Reid, R., Jin, G., Roy, B., Warren, M., 2017. Sampling a stimulated rock volume: An Eagle Ford example. In: SPE/AAPG/SEG Unconventional Resources Technology Conference. https://doi.org/10.15530/URTEC-2017-2670034.
Rein, R.G.J., Lord, D.L., Shah, S.N., 1993. Description of a large, high-pressure slot flow apparatus for characterizing fracturing fluids. In: SPE Annual Technical Conference and Exhibition. https://doi.org/10.2118/26524-MS.
Shrivastava, K., Hwang, J., Sharma, M., 2018. Formation of complex fracture networks in the Wolfcamp Shale: Calibrating model predictions with core measurements from the hydraulic fracturing test site. In: SPE Annual Technical Conference and Exhibition. https://doi.org/10.2118/191630-MS.
Thompson, R.L., Oishi, C.M., 2021. Reynolds and Weissenberg numbers in viscoelastic flows. J. Non-Newtonian Fluid Mech. 292, 104550. https://doi.org/10.1016/j.jnnfm.2021.104550.
Wang, B., Zhou, F., Zou, Y., Liang, T., Wang, D., Xue, Y., Gao, L., 2019. Quantitative investigation of fracture interaction by evaluating fracture curvature during temporarily plugging staged fracturing. J. Pet. Sci. Eng. 172, 559–571. https://doi.org/10.1016/j.petrol.2018.08.038.
Wang, B., Zhou, F., Yang, C., Wang, D., Yang, K., Liang, T., 2020a. Experimental study on injection pressure response and fracture geometry during temporary plugging and diverting fracturing. SPE J. 25, 573–586. https://doi.org/10.2118/199893-PA.
Wang, H., Sharma, M.M., 2018. Modeling of hydraulic fracture closure on proppants with proppant settling. J. Pet. Sci. Eng. 171, 636–645. https://doi.org/10.1016/j.petrol.2018.07.067.
Wang, J., Zhou, F., Bai, H., Li, Y., Yang, H., 2020b. A comprehensive method to evaluate the viscous slickwater as fracturing fluids for hydraulic fracturing applications. J. Pet. Sci. Eng. 193, 107359. https://doi.org/10.1016/j.petrol.2020.107359.
Wang, K., Wang, J., Hao, J., Shi, C., Pan, S., Marathe, S., Taylor, K.G., Ma, L., 2023. Nano-scale synchrotron imaging of shale swelling in the presence of water. Fuel 344, 127999. https://doi.org/10.1016/j.fuel.2023.127999.
Xu, B., Hill, A.D., Zhu, D., Wang, L., 2011. Experimental evaluation of guar-fracture-fluid filter-cake behavior. SPE Prod. Oper. 26, 381–387. https://doi.org/10.2118/140686-PA.
Yuan, B., Moghanloo, R.G., Zheng, D., 2016. Analytical evaluation of nanoparticle application to mitigate fines migration in porous media. SPE J. 21, 2317–2332. https://doi.org/10.2118/174192-PA.
Yuan, S., Zhou, F., Li, Y., Sheng, L., Liang, T., Tang, X., Liang, X., 2023. A comprehensive study on the enhancements of rheological property and application performances for high viscous drag reducer by adding diluted microemulsion. Geoenergy Sci. Eng. 227, 211770. https://doi.org/10.1016/j.geoen.2023.211770.
Zhang, D., Ma, S., Zhang, J., Zhu, Y., Wang, B., Zhu, J., Fan, X., Yang, H., Liang, T., 2022. Field experiments of different fracturing designs in tight conglomerate oil reservoirs. Sci. Rep. 12, 1–13. https://doi.org/10.1038/s41598-022-07162-y.
Zhang, J., Zhu, D., Hill, A.D., 2016. Water-induced damage to propped-fracture conductivity in shale formations. SPE Prod. Oper. 31, 147–156. https://doi.org/10.2118/173346-PA.
Zhao, X., Liang, T., Zan, J., Zhang, M., Zhou, F., Liu, X., 2021. Laboratory and pilot tests of enhanced oil recovery through wettability alteration by diluted microemulsions. In: SPE International Conference on Oilfield Chemistry. https://doi.org/10.2118/204291-MS.
Zhou, F., Su, H., Liang, X., Meng, L., Yuan, L., Li, X., Liang, T., 2019. Integrated hydraulic fracturing techniques to enhance oil recovery from tight rocks. Petrol. Explor. Dev. 46, 1065–1072. https://doi.org/10.1016/S1876-3804(19)60263-6.